Radar Returns from the Sea Surface—Bragg Scattering and Breaking Waves

O. M. PHILLIPS

Department of Earth and Planetary Sciences, The Johns Hopkins University, Baltimore, Maryland

(Manuscript received 15 June 1987, in final form 19 January 1988)

ABSTRACT

Recent ideas on the structure of the equilibrium range of wind-generated ocean waves are applied to the question of radar backscattered returns from the sea surface. It is shown that the backscattering cross section can be represented as the sum of separate contributions from Bragg-scattering and from individual breaking events:

$$\sigma_0 = \frac{\pi\beta}{2\sqrt{2}} |\cos\phi|^{1/2} \sin^{1/2}\theta \cot^4\theta F_1(\theta)\left(\frac{u_*^2\kappa}{g}\right)^{1/2} + F_2(\theta, \phi)\left(\frac{u_*^2\kappa}{g}\right)^{3/2}$$

where θ is the angle of incidence, ϕ is the direction of observation relative to the wind, u_* is the friction velocity and κ the radar wavelength; the Bragg-scattering contribution increases linearly with u_* and the sea spike contribution cubically. The number of sea spikes per unit time per unit surface area for a given threshold of spike intensity or duration is proportional to $g^{-1}u_*^3$. Calibrated radar measurements of median values of σ_0, which tend to suppress sea spike contributions, have been made by Guinard et al. over a range of radar wavelengths from 70 to 3.4 cm. These scale consistently with the parameter $(u_*^2\kappa/g)^{1/2}$ over angles of incidence greater than 30°, and are, overall, in accordance with a linear dependence. This suggests that the sea spike contribution to the median σ_0 is generally small over the range of observations, though their influence on the mean is not established. The cubic dependence predicted for the *frequency of occurrence* of sea spikes on u_* does, however, suggest a new and simpler method for the measurement of surface wind stress by remote sensing.

1. Introduction

The use of backscattered radar signals from the sea surface to provide reliable and accurate estimates of oceanic wind distributions has been regarded for almost twenty years as an essential aim of a global meteorological observational system. Satellite observations, in particular, provide the opportunity for rapid wind speed or wind stress measurements over wide areas of the ocean, invaluable for meteorological prediction purposes. The Seasat A Scatterometer System (SASS) was a strikingly successful demonstration that this goal might be attained provided the basic physics was clearly understood and the system could be properly calibrated. In order to establish empirically the dependence of the backscattering cross-section per unit area σ_0 of the sea surface upon the radar and environmental variables, many notable sets of measurements have been made, both from instrumented aircraft (for example, Guinard et al. 1971; Masuko et al. 1987) and from platforms (Chaudhry and Moore 1984, and others). Frequently, the variation of σ_0 with wind speed U is expressed by finding quantities G and H that give a best fit between the data and the formula (the "SASS-1 power law model")

$$\sigma_0 = G(p, f, \theta, \phi)U^{H(p,f,\theta,\phi)}. \tag{1.1}$$

The coefficient G and wind speed exponent H are taken to depend on the polarization, angle of incidence θ, (usually 20° or greater so that specular reflections are unimportant), radar frequency and direction of look ϕ relative to the wind.

Now as pointed out by Woiceshyn et al. (1986) in a careful, penetrating and ultimately very critical discussion of the present scatterometer wind retrieval system, Eq. (1.1), which is its basis, "is not a physical law, nor does it have any established scientific rationale". It is, of course, dimensionally inconsistent. Nevertheless, in an attempt to provide some empirical underpinning to (1.1), best-fit coefficients G and H have been calculated from various sets of measurements and a number of these have been summarized by Masuko et al. (1987). The wind speed coefficient H is of particular interest and Table 1 shows values of H that they report from measurements by different workers over a range of angles of incidence between 20° and 60°. The figures given are derived from data in which both transmitted and received signals were vertically polarized; the magnitudes and scatter in H from horizontally polarized signals are generally similar. The extent of the internal

Corresponding author address: Dr. O. M. Phillips, Dept. of Earth and Planetary Sciences, The Johns Hopkins University, Baltimore, MD 21218.

© 1988 American Meteorological Society

TABLE 1. Best-fit estimates of the wind speed coefficient H in Eq. (1.1); VV-polarization. The references are 1) Jones and Schroeder (1978), 2) Feindt et al. (1985), 3) Masuko et al. (1986), 4) Fung and Lee (1982), 5) Schroder et al. (1984), 6) Moore and Fung (1979), 7) Schroder et al. (1982).

Radar band	L			C		X						Ka
Radar frequency (GHZ)	0.428	1.228	4.45	5.3	8.91	10.0	13.3	13.9	13.9	13.9	14.6	34.4
Radar wavelength (cm)	70.1	24.4	6.73	5.65	3.7	3.0	2.25	2.16	2.16	2.16	2.05	0.87
Reference	1	1	1	2	1	3	1	4	5	6	7	3
Incidence angle												
20°	—	—	—	0.6 (18°) 1.0 (25°)	—	0.65 (22°)	1.12 1.10 (25°)	—	0.87	—	0.98	0.34 (22°)
30°	0.69 0.34	1.47 0.55	1.20 0.91 1.28	1.4 (35°)	1.10 0.95 1.20	1.70	1.49 1.42 (35°)	1.39 1.61 (32°)	1.40	1.88	1.54	1.49
40°	—	—	1.50 (45°)	1.4 (45°)	0.9 (45°)	1.98	—	1.89 1.36 (43°)	2.04	2.18	1.71	1.29
50°	—	—	—	1.4 (55°)	—	2.24	—	1.69 1.32	2.17	2.36	1.72	1.79
60°	—	—	1.30	—	1.35	2.30	—	—	0.72	—	1.72	1.88

inconsistencies is striking. To be sure, intensity measurements of the kind involved here are difficult, and involve problems of calibration, "ground truth" (the comparison of measurements over an area as made by radar with those at a fixed location in a naturally varying environment) and averaging times that are not as long as one would like (particularly in aircraft measurements). Furthermore, the numbers in Table 1 are obtained frequently by fitting (1.1) to only a few discrete measurements at different wind speeds, different observers in many cases covering different ranges. Although one's confidence in the individual values of Table 1 is low, it does appear that most of the values of H lie in the range 0.8 to about 1.5 except for the higher frequencies (X-band) *and* larger angles of incidence (40° and above) when values of two or more appear. For the purpose of processing scatterometer measurements, so-called G–H tables have been developed (for example, Schroeder et al. 1982, p. 3322) from these kinds of data giving interpolated and smoothed values to an apparent four-digit accuracy!

Efforts to understand the physical processes at the sea surface that are responsible for these return signals have been made for over thirty years, but the goal of providing a better based, more general and more accurate representation than (1.1) has remained elusive. Already by 1955, Crombie had observed Bragg resonances in wind-wave systems and Wright (1966) and Wright and Keller (1971), using Doppler radar measurements in a wind-wave tank, showed conclusively that substantial signals were obtained from scattering elements that moved with phase speeds equal to the phase speeds of surface waves whose wavenumber k was that associated with first-order Bragg scattering, i.e.

$$k = 2\kappa \sin\theta, \tag{1.2}$$

where κ is the radar wavenumber and θ the angle of incidence. If the sea surface can be represented as a superposition of random wave components of infinitesimal slope and with a two-dimensional spectrum $\Psi(\mathbf{k})$ such that $\Psi(\mathbf{k}) = \Psi(-\mathbf{k})$ with the mean square surface displacement

$$\bar{\zeta}^2 = \int \Psi(\mathbf{k})d\mathbf{k},$$

then the backscattering cross section per unit area of the surface is given by the well-known Bragg expression (e.g., see Valenzuela 1978; Brekhovskikh and Lysanov 1982)

$$\sigma_0 = 4\pi\kappa^4 \cos^4\theta F_1(\theta)\Psi(2\kappa \sin\theta, 0). \tag{1.3}$$

In this equation, $F_1(\theta)$ depends on the polarization of the transmitted and received signals, the form being given explicitly by Wright (1966), Saxon and Lane (1952), and Valenzuela (1978); the backscattered signal is provided by only that component of the surface wave spectrum specified by the Bragg resonance condition (1.2).

If first-order Bragg scattering represents the dominant contribution to the return signal, then the variation of σ_0 with wind speed reflects that of the spectral density Ψ at the appropriate wavenumber. Until recently it had been believed that the form of the surface wave spectrum in the gravity wave range was determined by a saturation process (Phillips 1958) and that the spectral density was independent of wind speed under saturation conditions. This is flatly inconsistent with the results of Table 1, which, rough though some of them may be, do indicate clearly that σ_0 increases

with wind speed. The approximations implicit in (1.3) have been examined carefully by Valenzuela (1978) and others; the presence of swell in causing tilt and slope of the local surface containing the scattering wavelets and in interacting with these wavelets does modulate the local σ_0, but the overall spatial average is changed only at the second order of the (small) rms wave slope $[\overline{(\nabla\zeta)^2}]^{1/2}$. However, the most reliable radar measurements were (and still are) at frequencies about 10 GHz and above (X and Ka bands, radar wavelengths less than 3 cm) where the surface waves responsible for Bragg scattering become increasingly influenced by capillarity and molecular viscosity and hence water temperature; the applicability of the saturation-range ideas to these frequencies was certainly in doubt. The inconsistency at lower radar frequencies remained, but we learned to live with it.

There are good observational indications that not all of the return signals are produced by Bragg scattering, particularly at near normal incidence, incidence angles less than 30° or so, when specular returns are large and also at large incidence angles and high frequencies. Kalmykov and Pustovoytenko (1976) with X-band (3.2 cm) radar at large incidence angles detected "bursts", sporadic, intermittent patches of high intensity returns superimposed on the more general, presumably Bragg-type, signal. Particularly evident with horizontally polarized radar, these returns, commonly called "sea spikes" have been associated by Wetzel (1986) and others with individual breaking events. Wetzel has constructed an idealized model based on the breaking plume description of Longuet-Higgins and Turner (1974) that predicted radar cross sections from individual events of the order of magnitude observed (one or a few square meters), but there seem to have been no published quantitative measurements or estimates of their relative contribution to the overall signal or variation with wind speed and radar wavelength. Indeed, Chaudry and Moore (1984), recognizing sea spikes as non-Gaussian contributions to the return signals, went to extraordinary lengths to remove them from their data, rather than accepting them as an intrinsic and possibly important part of the measurement.

The primary obstacle to a quantitative understanding of these experimental results seems now to have been a lack of understanding (and, in part, a positive misunderstanding) of the statistical and spectral properties of short gravity waves and breaking waves on the sea surface. The purpose of this paper is to seek more quantitative connections between recently developed concepts of the short-wave spectral structure and statistics of breaking in wind-generated waves on the one hand and, on the other, the more detailed and precise radar backscattering measurements that have become available. As it will appear, the connections can now be made much tighter than was possible before, though some possibly significant discrepancies remain and some important phenomena such as the spectral structure of gravity–capillary and capillary waves remain unexplored. Nevertheless, the hope is to provide a better framework for the analysis of these radar measurements under relevant conditions and, in consequence, to give to the oceanographer greater credibility to radar techniques in the measurement of specific characteristics of the sea surface.

2. The double structure of sea surface scatterers

When the wind blows over the sea surface, it generates a distribution of waves of generally small slope that propagate and interact weakly with one another. If the energy input from the wind continues for a sufficient time, sporadic breaking events occur on a variety of scales from microscale breaking with capillary wavelets to small splashing events to larger ones in which air entrainment is vigorous and whitecaps are formed. In these isolated sporadic events, which appear and disappear, the local surface slope is not small throughout the history of each one—at any instant they represent isolated steep convolutions of the surface superimposed on an overall wavy background of small slope. At any instant in time, if there are no ocean current or topographic effects, active wave-breaking events appear to be randomly distributed in space and generally separated by distances large compared with the dominant wavelength of the wave field, the specific pattern of breakers changing constantly in time as they are born, develop, advance, and decay.

Now, suppose this scene is illuminated by radar of a particular wavelength and angle of incidence θ which is sufficiently large that specular reflections, except possibly from breaking events, are unlikely. Except at grazing incidence, most of the radiant energy is incident on the surface covered by waves of small slope and a backscattered signal is produced by the component of the surface wave spectrum with wavenumber k specified by the Bragg condition (1.2). In addition, isolated small regions where wave breaking is occurring with a locally steep, convoluted configuration, produce pulse returns as would any other localized target. In this type of return, there is no tight association between the scale of the target and the wavelength of the scattered radiation as there is in Bragg scattering, so that a given radar frequency can detect the local targets represented by wave breaking over a considerable range of scales. If the scale, h, of the breaking zone is very large compared with the radar wavelength, λ, the return signal approaches what might be considered the optical or geometrical limit, but as we shall see, large breaking events are relatively rare. When the scale is very small compared with the radar wavelength, the scattered return approaches the Rayleigh limit, decreasing as $(h/\lambda)^4$. For wave breaking events generating sea spikes, h/λ lies between these limits.

Since the individual breaking events at any instant are distributed apparently randomly over the surface

with distances between them large compared with the radar wavelength, the return signals will have random phase and so will add in mean square. Moreover, the distribution of breaking events over the range of scales detected by the radar should be independent of the spectral density of the wave field at the particular wavenumber that is Bragg resonant (unless, conceivably but rarely, this happens to be the dominant wavenumber of the wave field). Accordingly, the separate contributions from Bragg backscattering and from the localized breaking-wave sources, the sea spikes, will also add in mean square. The backscattering cross section per unit area of the sea surface, proportional to the ratio of the return power to transmitted power, is then the sum of the separate contributions from the two:

$$\sigma_0 = \sigma_B + \sigma_{ss}. \tag{2.1}$$

The Bragg contribution σ_B is given by Eq. (1.3), where Ψ is the surface wave spectral density. As mentioned previously, it had been believed that under an active wind, the spectral density for gravity wave components saturated at a level independent of u_*, the friction velocity of the wind. Recently, however, a more detailed dynamical analysis (Phillips 1985) has shown that for wavenumbers k in the gravity range whose propagation speed is not small compared with u_*, i.e.

$$k_0 \ll k < \min\{(g/\gamma)^{1/2}, g/u_*^2\}, \tag{2.2}$$

where k_0 is the wavenumber of the spectral peak and γ is the surface tension divided by water density, the wave spectral density under equilibrium conditions is

$$\Psi(\mathbf{k}) = \beta|\cos\phi|^{1/2} u_* g^{-1/2} k^{-7/2}, \tag{2.3}$$

where $\beta \sim 10^2$ and ϕ is the angle between the wavenumber $\mathbf{k}$ and the wind. [The directional distribution in nature is certainly "smoothed out" near $\phi = \pm\pi/2$ and may be enhanced near $\phi = 0$ by the turning effects of long waves; the definition is such that $\Psi(\mathbf{k}) = \Psi(-\mathbf{k})$.] Other predictions from this analysis compare well with experiment, though there has yet been only scanty direct confirmation of the specific result (2.3). If, however, this is substituted into (1.3), we obtain for the Bragg backscattering cross section per unit area

$$\sigma_B = 2^{-3/2}\pi\beta|\cos\phi|^{1/2}\sin^{1/2}\theta\cot^4\theta F_1(\theta)\left(\frac{u_*^2\kappa}{g}\right)^{1/2}, \tag{2.4}$$

provided

$$2\kappa\sin\theta < \min\{(g/\gamma)^{1/2}, g/u_*^2\}. \tag{2.5}$$

For a given radar frequency (and so wavenumber κ), angle of incidence θ and angle ϕ to the wind, σ_B increases linearly with friction velocity u_*, provided (2.5) is satisfied.

The situation when the inequality (2.5) is not satisfied is far from clear. In very light winds, the extent of the equilibrium range specified by (2.2) may be too small to allow a significant range of validity of (2.3). Under high wind stress, when $g/u_*^2 \ll (g/\gamma)^{1/2}$, or $u_* \gg (\gamma g)^{1/4}$ there is some evidence (Phillips 1985) that short gravity waves are suppressed so that one might expect σ_B to be less than that given by (2.4). Trains of capillary waves generated by the wind over the longer gravity waves will provide Bragg backscattering at frequencies in the high X-band and Ka band (radar wavelengths 1–2 cm), but the form of the mean capillary wave spectrum and even the processes that determine its equilibrium, remain unknown.

In addition, we have the contributions from the localized breaking-wave sources, the sea spikes discussed by Wetzel, and to find this we need information on the density of wave breaking on the sea surface as a function of scale and friction velocity u_*. There are some conceptual difficulties in making a precise definition of the scale of a breaking wave in a way that allows direct measurement, but the velocity $\mathbf{c}$ of the breaking front does provide a measure of the scale that could in principle be found from a movie or video record of the sea surface. Accordingly, let us define $\Lambda(\mathbf{c})d\mathbf{c}$ as the average total length of breaking fronts per unit surface area that have velocities of advance in the range $\mathbf{c}$ to $\mathbf{c} + d\mathbf{c}$. Since $\mathbf{c} = \mathbf{c}(\mathbf{k})$, the average total length of breaking front per unit surface area associated with wavenumbers in the range $\mathbf{k}$ to $\mathbf{k} + d\mathbf{k}$ is

$$\Lambda(\mathbf{k}) = \Lambda(\mathbf{c})\frac{\partial(c_1, c_2)}{\partial(k_1, k_2)}.$$

(For the larger scale breaking events, $c = (g/k)^{1/2}$ but if short-wave breaking occurs only at the crests of longer waves or swell, allowance must be made for the long-wave advection). Now, as pointed out in an earlier paper (Phillips 1985), the rate of energy dissipation per unit length of a breaking wave with intrinsic speed c is proportional to c^5/g or $g^{3/2}k^{-5/2}$, so that the spectral rate of energy loss from the wave field by breaking can be represented as

$$\epsilon(\mathbf{k}) \propto g^{3/2}k^{-5/2}\Lambda(\mathbf{k}).$$

Finally, in the same paper, it was shown by considering the spectral energy balance in the equilibrium range that $\epsilon(\mathbf{k})$ could also be represented in terms of the friction velocity of the wind as

$$\epsilon(\mathbf{k}) \propto |\cos\phi|^{3/2}u_*^3k^{-2}.$$

Equating these two expressions gives for the distribution with respect to wavenumber $\mathbf{k}$, of expected length of breaking front per unit surface area,

$$\Lambda(\mathbf{k}) = \text{const}|\cos\phi|^{3/2}g^{-3/2}k^{1/2}u_*^3, \tag{2.6}$$

provided k satisfies the restriction (2.2).

Now, the scattering of radar waves incident on a

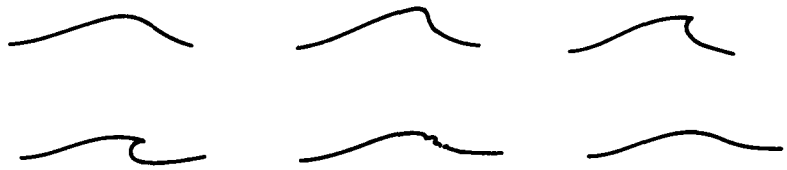

FIG. 1. A sequence of profiles in an individual breaking wave.

local surface convolution depends in a very complicated way on the geometry of the convolution, its scale relative to the radar wavelength and the angle of incidence. As illustrated in Fig. 1, in each breaking event, the surface passes through a sequence of configurations before it disappears and at any instant, a large area of the surface illuminated by the radar will, at each scale, include samples of these configurations with equal probability throughout the event, since they occur randomly. If the height, h, of the breaking zone is sufficiently large that capillarity is unimportant, i.e., if $h > (\gamma/g)^{1/2}$, we can assert that breaking is an unsteady, inviscid, gravity-dominated flow in which the geometries of the sequences of breaking events are independent of scale h. The scattered wave pattern can then depend on scale only through the combination κh, where κ is the radar wavenumber. Consequently, the radar cross section per unit area produced by breaking waves with wavenumbers in the range $\mathbf{k}$, $\mathbf{k} + d\mathbf{k}$ must be equal to the expected geometrical area of the scatterers associated with this wavenumber interval, $h\Lambda(\mathbf{k})d\mathbf{k}$ times some dimensionless function of κh, the angle of incidence θ, and the azimuth angle to the wind ϕ; this function depends in turn on the family of surface configurations represented in the breaking events. Note that we do not wish to describe the scattering in terms such as "specular" or "wedge scattering" as has sometimes been suggested; although these terms may be appropriate at specific instants in each configuration, we consider the overall contribution of the family of configurations at different scales presented by the breaking histories. The total cross section per unit area produced by breaking at all scales, the "sea spike" contribution, is then

$$\sigma_{ss} = \int h\Lambda(\mathbf{k})f_1(\kappa h, \theta, \chi)d\mathbf{k}, \qquad (2.7)$$

provided $h > (\gamma/g)^{1/2} \sim 0.3$ cm for an air–water interface. Since under these conditions, the scale height, h, of the breaking front is proportional to the wavelength of the wave itself, or to k^{-1},

$$\sigma_{ss} = \int k^{-1}\Lambda(\mathbf{k})f_2(k/\kappa, \theta, \chi)d\mathbf{k}, \qquad (2.8)$$

where $k/\kappa \propto \lambda/h$ the ratio of the radar wavelength to the scale height of a breaker.

The integration in (2.8) is over the wavenumbers of the equilibrium range, that is, over wavenumbers larger than that of the spectral peak (k_0) yet satisfying (2.2). Now most radar observations have been made at X-band frequencies or less, that is, radar wavelengths of 3 cm or more, which is at least an order of magnitude larger than the scale h of the smallest breaking waves whose geometries may be strongly influenced by surface tension. The integration of (2.8) is then limited at high wavenumbers by the Rayleigh cutoff with $f_2 \propto (k/\kappa)^{-4} \propto (\lambda/h)^{-4}$, which decreases rapidly when $\lambda \gg h$, i.e., by the inability of the radar to detect the smallest scales rather than by the equilibrium range limitations on $\Lambda(\mathbf{k})$, so that the upper limit of integration for k can be taken as infinite without serious error. The substitution of (2.6) into (2.8) and integration over the direction ϕ then gives

$$\sigma_{ss} = u_*^3 g^{-3/2} \int_{k_0}^{\infty} k^{1/2} f_3(k/\kappa, \theta, \chi)dk$$
$$= \left(\frac{u_*^2\kappa}{g}\right)^{3/2}\left\{\int_0^{\infty} - \int_0^{k_0/\kappa} x^{1/2} f_3(x)dx\right\}, \qquad (2.9)$$

where $x = k/\kappa$ and the dependences on θ and χ are to be understood. Now in oceanic circumstances in which scattering from breaking waves may be significant (at least moderate wind speeds and fetches, and so moderately long dominant waves; high frequency radar) the scale h_0 of the largest breaking events is considerably larger than the radar wavelength, so that $h_0\kappa \gg 1$, $k_0/\kappa \ll 1$ and the function f_3 is approximately constant in the range $(0, k_0/\kappa)$. Consequently, (2.9) reduces to

$$\sigma_{ss} = F(\theta, \chi)\left(\frac{u_*^2\kappa}{g}\right)^{3/2}\{1 - O(k_0/\kappa)^{3/2}\}. \qquad (2.10)$$

A calculation of the form of the function $F(\theta, \chi)$ would require analysis of the scattering from the family of three-dimensional local surface configurations involved in wave breaking and this will not be attempted here. One would anticipate, however, that the dependence on χ, look angle relative to the wind, would be stronger than in Bragg scattering, and that, when looking upwind, F would increase with angle of incidence θ, and, at given θ, would be larger when looking upwind than when looking downwind.

Since the numerical values of χ in (2.10) and ϕ in (2.4) are the same, the combined backscattering cross section σ_0 per unit surface area is then the sum of (2.4) and (2.10):

$$\sigma_0 = \frac{\pi\beta}{2\sqrt{2}} |\cos\phi|^{1/2} \sin^{1/2}\theta \cot^4\theta F_1(\theta)\left(\frac{u_*^2\kappa}{g}\right)^{1/2} + F_2(\theta, \phi)\left(\frac{u_*^2\kappa}{g}\right)^{3/2}. \quad (2.11)$$

The primary condition for the validity of the first term is given by (2.5) (i.e., Bragg scattering from short gravity wave components) and for that of the second term, $k_0/\kappa \ll 1$ (i.e., radar wavelengths small compared with the scale height of the largest breaking waves). The relative magnitudes of the functions F_1 and F_2 is, a priori, unknown.

3. The frequency per unit area of breaking events

Individual breaking events are fugitive and sporadic; the radar sea spikes associated with them are transient. Kalmykov and Pustovoytenko (1976) reported that the duration of the individual "bursts" they recorded was between 0.1 and 0.3 s with a 3.2 cm radar at glancing incidence in a sea state 3–4 with a median wave height 2–2.5 m. Evidently the primary, most intense return is derived from a short time interval in the evolution sequence illustrated in Fig. 1; it is of interest to inquire about the expected frequency per unit area with which such events occur and the dependence of this frequency upon wind speed.

The total length per unit area associated with wavenumbers in the range $\mathbf{k}, \mathbf{k} + d\mathbf{k}$ is $\Lambda(\mathbf{k})d\mathbf{k}$, and because of the geometrical similarity expected, the average length of each breaking segment is proportional to k^{-1}. Consequently the number of individual segments per unit area at any instant is proportional to $k\Lambda(\mathbf{k})d\mathbf{k}$. The lifetime of each event and so the duration of each spike is, for the same reason, proportional to (but a smallish fraction of) the wave period n^{-1} so that the expected number of events appearing (and disappearing) per unit area per unit time is this number density divided by the lifetime, or $nk\Lambda(\mathbf{k})d\mathbf{k}$:

$$\nu(\mathbf{k})d\mathbf{k} \propto nk\Lambda(\mathbf{k})d\mathbf{k}. \quad (3.1)$$

If we consider the larger scale breakers producing the more intense sea spikes, the advection by the orbital velocity of longer waves is of lesser significance and $n \approx (gk)^{1/2}$ and (3.1) reduces to

$$\nu(\mathbf{k})d\mathbf{k} \propto g^{1/2}k^{3/2}\Lambda(\mathbf{k})d\mathbf{k} \propto |\cos\phi|^{3/2} g^{-1}k^2u_*^3 d\mathbf{k}, \quad (3.2)$$

from (2.6). The total number of breaking events per unit area per unit time associated with waves whose wavenumbers lie between k_0, that of the spectral peak, and k_1, some upper limit, is therefore

$$\nu(k_0, k_1) = \int_0^{2\pi}\int_{k_0}^{k_1} \nu(\mathbf{k})d\mathbf{k} \propto g^{-1}u_*^3(k_1^4 - k_0^4). \quad (3.3)$$

Now, in a radar measurement of sea spikes, suppose we count only those events whose intensity or whose duration exceeds some convenient threshold that enables them to be identified unambiguously. Since the threshold intensity and duration both increase monotonically with increasing wavelength, either choice corresponds to a threshold wavenumber k_1 below which the associated sea spikes will be identified; if in a reasonably well-developed sea state, this wavenumber is substantially larger than that of the spectral peak, $k_1^4 \gg k_0^4$ and (3.3) reduces to

$$\nu(k_1) \propto g^{-1}k_1^4u_*^3. \quad (3.4)$$

When the radar-scanned area A is such that few of the intervals of intensive return overlap, the total number of sea spikes recorded per unit time for a fixed threshold is $\nu(k_1)A$.

4. Comparisons with radar measurements

It is interesting to note even at this stage that the qualitative trends for the "wind speed exponent" of Table 1 are not inconsistent with the prediction (2.11). At large incidence angles and small radar wavelengths, H is generally large; if the second term in (2.11) dominated, it should approach 3. Otherwise, when Bragg scattering predominates, the exponent should be close to unity. However, many of the sets of measurements summarized in Table 1 are relative measures at different wind speeds (the numerical values of σ_0 involve an arbitrary multiplicative constant) rather than absolute measures in which the system was calibrated using the return from a known scattering object of simple geometry. As a result, it is not possible in most instances to compare directly the actual data points from different sets. There is, however, one important set of published data obtained by Guinard et al. (1971) using four different radar frequencies from 0.4 to 9 GHz over a range of wind speeds, that is carefully calibrated so that measurements at different radar frequencies can be intercompared. These results, about 20 years old, report values of cross section σ_0 that are *median* rather than mean values. The Bragg contribution to the total return signal is approximately Gaussian and for this part, the median and the mean are approximately the same. Superimposed on this, however, is the sea spike contribution with sporadic short intervals of potentially much greater intensity. If the fraction of the total observation time occupied by sea spike returns is small, their influence on the *median* is small, no matter how great their intensity. Such measurements therefore tend to suppress the sea spike contribution relative to the Bragg contribution, so that a priori one would expect to find a linear dependence on $(u_*\kappa^{1/2}g^{-1/2})$. The Guinard et al. measurements were obtained from aircraft with relatively short averaging times and therefore have a good deal of scatter, but nevertheless, when viewed as a whole, they will be

seen to provide striking support for a dependence of σ_0 on $(u_* \kappa^{1/2} g^{-1/2})$ that is, within experimental accuracy, linear over the range of observational conditions.

These measurements were made near ocean weather stations India and Juliet in the North Atlantic Ocean, which provided wind speed, direction, and gross wave information. All were made in the upwind direction. Individual values of the median normalized cross sections σ_0 measured at the four frequencies for various angles of incidence and wind speeds were read from enlarged prints of their diagrams. No wind profile measurements were available and the results are not categorized quantitatively in terms of air–sea temperature differences, so that their quoted values of wind speed were converted to u_* using a drag coefficient of 1.5×10^{-3} at the higher wind speeds (11–24 m s^{-1}) and 10^{-3} at 2.5 m s^{-1}. The values of σ_0 were then replotted in terms of $(u_* \kappa^{1/2}/g^{1/2})$ for the various angles of incidence between 30° and 85° and for HH and VV polarizations.

The results are shown in Figs. 2a to 2l. Results from incidence angles 0° and 15° are not shown; the return at these angles is primarily specular. It is evident from these figures that the results at the different radar frequencies do form clouds in which the scatter of σ_0 values is generally no greater than it is in the individual sets of measurements at each frequency, and so are consistent with a scaling of the form

$$\sigma_0 = \text{function}\left(\frac{u_* \kappa^{1/2}}{g^{1/2}}\right). \tag{4.1}$$

The measurements at the lowest wind speed (nominally 2.5 m s^{-1}), represented by the three left-hand-most points in each figure tend to scatter more widely than the others, presumably as a result of low wind speed variability. The line in each figure drawn through the points corresponds to a linear dependence of σ_0 upon $(u_* \kappa^{1/2}/g^{1/2})$ and the measurements are generally within ±3 dB of these lines. The results for VV polarization at 70° and 80° incidence angles are somewhat more scattered than the others and the "best fit" slope for HH polarization at 70° would be larger than unity, but if the low P-band measurements are ignored, the linear dependence fits well. The HH results at 60°, 80° and 85° give no hint of a larger slope.

It is clear from an examination of these figures that the measurements made at each separate frequency and angle of incidence do not individually define a wind speed dependence—the scatter in the four or five points is too great. Nevertheless, the values in Table 1 are derived from individual sets such as these by least-squares fitting. Only when the results from different radar wavelengths are plotted together does any consistent pattern emerge. Any one of these figures 2a–l indicates that the results do group according to (4.1) and suggests that the functional dependence is close to linear. The fact that *all* of the results at different polarizations and angles of incidence group close to the same slope is, to this author, persuasive evidence that the dependence of σ_0 on $(u_* \kappa^{1/2} g^{-1/2})$ is indeed linear over this range. There is no real indication of a steeper slope at the larger values of $(u_* \kappa^{1/2} g^{-1/2})$ and larger angles of incidence, so that the contribution to the overall median σ_0 from sea spikes associated with breaking waves seems insignificant. These measurements are intrinsically unable to resolve the question of the contribution of sea spikes to the *mean* σ_0, so that the influence of the final term in (2.11) remains unexamined. The fact, however, that the values of H in Table 1, obtained by fitting a single power, are consistently greater than unity is consistent with the polynomial expression (2.11). There is, in fact, possibly a hint of saturation in some of the figures at large values of $(u_* \kappa^{1/2} g^{-1/2})$, but it is far from clear. Apparently the inequality (2.5) does not have to be satisfied strongly for the Bragg backscattering expression (2.4) to be reasonably accurate.

In section 3, an expression is offered for the frequency of occurrence of sea spikes generated per unit area of the sea surface, but there seem to be no published measurements yet available with which it can be compared. The predicted cubic dependence on u_* for a given threshold is however interesting, and raises the possibility that, if the general form (3.4) could be confirmed experimentally, a more sensitive and potentially simpler method for the measurement of wind stress (particularly larger values) could be developed using counting techniques rather than intensity measurements.

5. Conclusions

The measurements discussed in the previous section confirm (i) that over the range of angles of incidence between 30° and 85°, the backscattered cross section scales with friction velocity and radar wavenumber as functions of $u_* \kappa^{1/2} g^{-1/2}$, indicating the applicability of equilibrium range ideas; (ii) that the dependence is close to the linear form predicted for Bragg scattering alone.

It would be extremely valuable if systematic high quality data at high incidence angles were available on the frequency of occurrence of sea spikes. Three basic physical problems are associated with the use of Bragg scattering returns for the measurement of wind speed. First, intensity measurements to an accuracy of ±1 dB or so, as are required, are extremely difficult to make, and subject to attenuation and other corrections. Second, the measurement is spectrally specific, and the measurement of the spectral density of a particular component of a random sea to a given accuracy requires very large samples, with consequent degradation of spatial/temporal resolution. Third, when $u_* \kappa^{1/2} g^{-1/2}$ exceeds about 2, the physics of the surface waves involved in Bragg returns becomes very complicated and

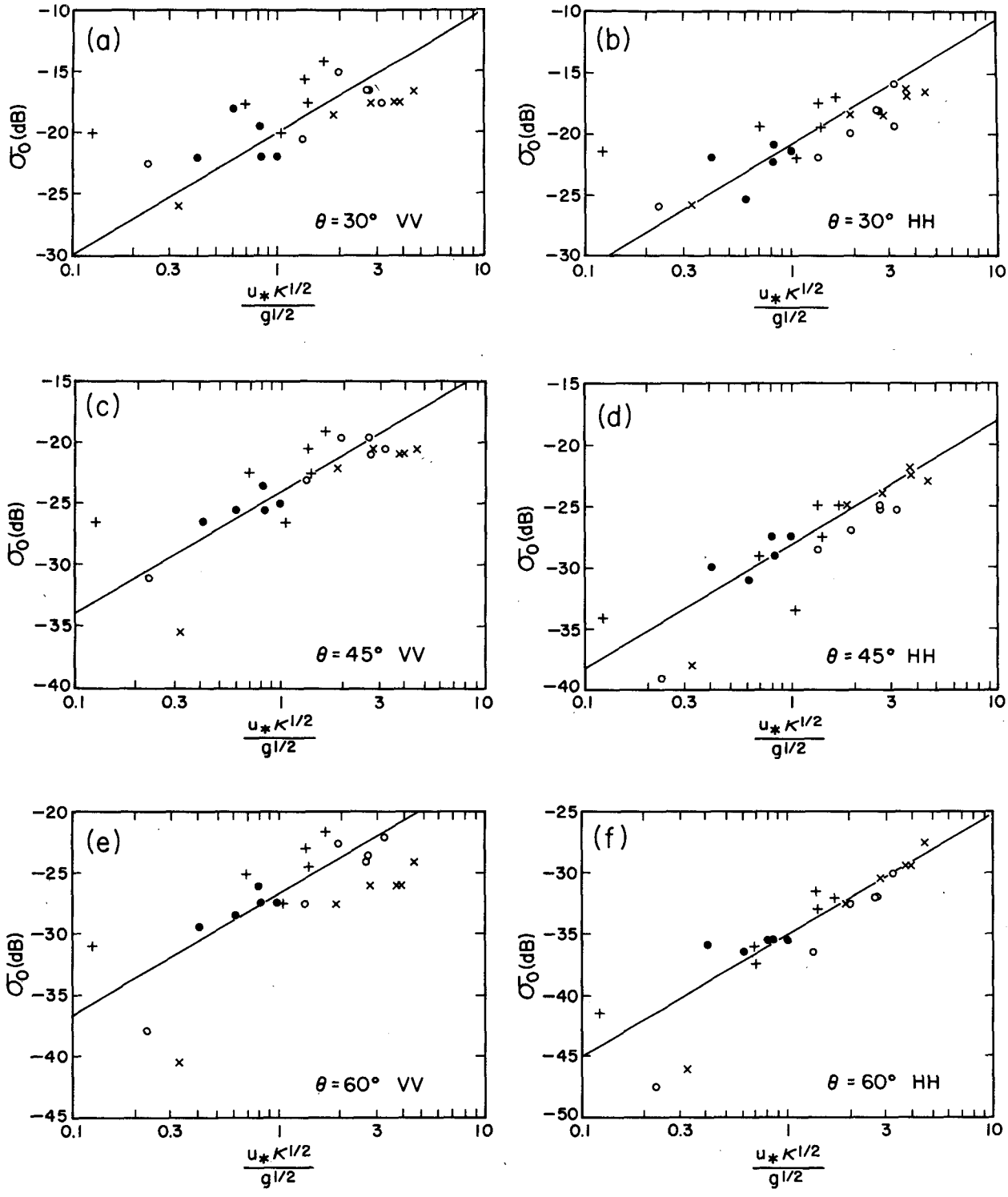

FIG. 2. The dependences of median σ_0 on $(u_* \kappa^{1/2} g^{-1/2})$ at various angles of incidence and for VV and HH polarizations, as measured by Guinard et al. (1971). Wind speeds range from 2.5 to 24 m s^{-1}; measurements taken during snow are not plotted. ×: X-band, 8.91 GHz, radar wavelength 3.4 cm; O: C-band, 4.45 GHz, 6.9 cm; +: L-band, 1.228 GHz, 24 cm and ●: P-band, 0.428 GHz, 70 cm.

obscure, involving additional surface and fluid problems, and the behaviour of σ_0 becomes very ragged. Unfortunately this range corresponds to high wind conditions in which the accurate determination of u_* is most important in many applications. It would, in principle, be possible to use substantially smaller radar

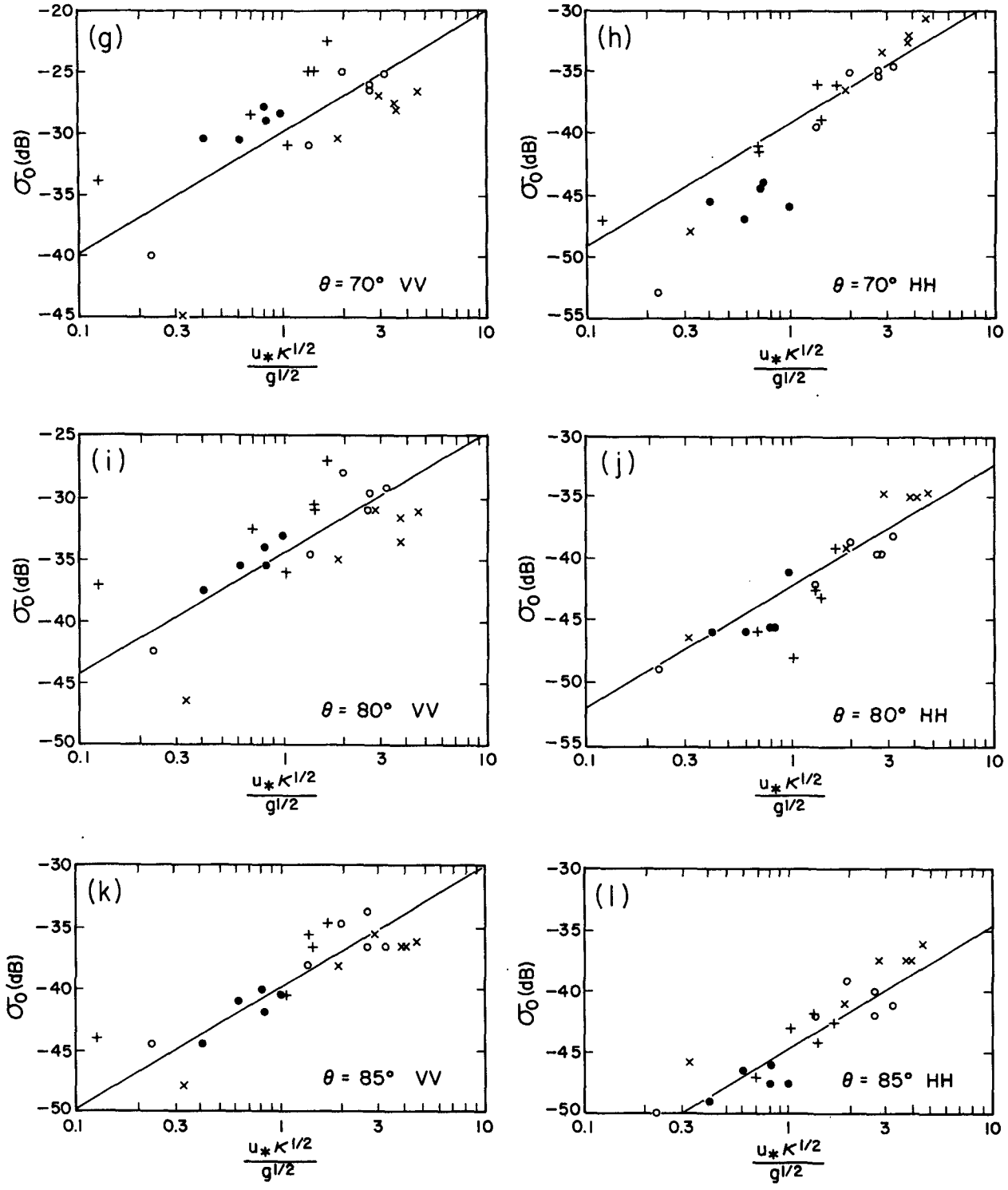

FIG. 2. (*Continued*)

wavenumbers, lower frequencies than the 5–10 GHz range now used, in order to keep the operating range within the apparently better defined linear region, but this would require larger antennas that are very undesirable in satellite operations.

An alternative procedure would be to take advantage of the sea spike returns, rather than trying to suppress them. Counting techniques are intrinsically simpler than intensity measurements, and if at the *larger* incidence angles where ordinary specular reflections are

negligible, a suitable threshold can be found to give unambiguous identification of spikes with a sufficient sampling rate (the Bragg-type returns might be suppressed by filtering), Eq. (3.4), suitably calibrated, would allow u_* to be measured. Other advantages associated with this proposed technique are that it would (i) have a stronger u_* dependence (cubic) allowing better discrimination particularly at high u_* values, (ii) not be spectrally specific, but depend on the integral effect of all breaking scales above that associated with the chosen threshold and consequently be insensitive to surface properties and small-scale surface wave processes and (iii) provide stronger directional response with a probably strong upwind–downwind asymmetry allowing wind directions to be determined without ambiguity. Before this suggestion can be implemented, however, more high quality measurements at larger incidence angles are necessary.

Acknowledgments. I am particularly grateful to Professor Werner Alpers and Dr. William Keller for their helpful discussion of this work, and to Professor Klaus Hasselmann for his hospitality at the Max-Planck Institut für Meteorologie, Hamburg University, during my sabbatical leave when much of this work was done. The research was supported by the Office of Naval Research under Contracts N00014-76-C-0184 and N00014-87K-0412.

REFERENCES

Brekhovskikh, L., and Yu. Lysanov, 1982: *Fundamentals of Ocean Acoustics.* Springer-Verlag.

Chaudhry, A. H., and R. K. Moore, 1984: Tower-based backscatter measurements of the sea. *IEEE J. Ocean. Eng.,* **OE-9,** 309–316.

Crombie, D. D., 1955: Doppler spectrum of sea-echo at 13.56 mc/s. *Nature,* **175,** p. 681.

Feindt, F., V. Wisman, W. Alpers and W. C. Keller, 1985: Airborne measurements of the ocean radar cross-section at 5·3 GHz. *Radio Sci.,* **21,** 845–856.

Fung, A. K., and K. K. Lee, 1982: A semi-empirical sea-spectrum model for scattering coefficient estimation. *IEEE J. Ocean. Eng.,* **OE-7,** 166–176.

Guinard, N. W., J. T. Ransone and J. C. Daley, 1971: Variation of the NRCS of the sea with increasing roughness. *J. Geophys. Res.,* **76,** 1525–1538.

Jones, W. L., and L. C. Schroeder, 1978: Radar backscatter from the ocean: dependence on surface friction velocity. *Bound.-Layer Meteor.,* **13,** 133–149.

Kalmykov, A. I., and V. V. Pustovoytenko, 1976: On polarization features of radio signals scattered from the sea surface at small grazing angles. *J. Geophys. Res.,* **81,** 1960–1964.

Longuet-Higgins, M. S., and J. S. Turner, 1974: An 'entraining plume' model of a spilling breaker. *J. Fluid Mech.,* **63,** 1–20.

Masuko, H., K. Okamoto, M. Shimada and S. Niwa, 1986: Measurements of microwave back-scattering signatures of the ocean surface using X-band and Ka-band airborne scatterometers. *J. Geophys. Res.,* **91,** 13 065–13 083.

Moore, R. K., and A. K. Fung, 1979: Radar determination of winds at sea. *Proc. IEEE,* **67,** 1504–1521.

Phillips, O. M., 1958: The equilibrium range in the spectrum of wind-generated ocean waves. *J. Fluid Mech.,* **4,** 426–434.

——, 1985: Spectral and statistical properties of the equilibrium range in wind-generated gravity waves. *J. Fluid Mech.,* **156,** 505–531.

Saxon, J. A. and J. A. Lane, 1952: Electrical properties of sea water. *Wireless Eng.,* **291,** 269–275.

Schroeder, L. C., D. H. Boggs, G. Dome, I. M. Halberstam, W. L. Jones, W. J. Pierson and F. J. Wentz, 1982: The relationship between wind vector and normalized radar cross section used to derive SEASAT-A satellite scatterometer winds. *J. Geophys. Res.,* **87,** 3318–3336.

——, W. L. Jones, P. R. Schaffner and J. L. Mitchell, 1984: Flight measurements and analysis of AAFE RADSCAT wind speed signature of the ocean. NASA Tech. Memo. TM-85646.

Valenzuela, G. R., 1978: Theories for the interaction of electromagnetic and oceanic waves—a review. *Bound.-Layer Meteor.,* **13,** 61–85.

Wetzel, L., 1986: On microwave scattering by breaking waves. *Wave Dynamics and Radio Probing of the Ocean Surface,* O. M. Phillips and K. Hasselmann, Eds., Plenum, 273–284.

Woiceshyn, P. M., M. G. Wurtele, D. H. Boggs, L. F. McGoldrick and S. Peteherych, 1986: The necessity for a new parametrization of an empirical model for wind/ocean scatterometry. *J. Geophys. Res.,* **91,** 2273–2288.

Wright, J. W., 1966: Backscattering from capillary waves with application to sea clutter. *IEEE Trans. Antennas Propag.,* **14,** 217–233.

——, and W. C. Keller, 1971: Doppler spectra in microwave scattering from wind waves. *Phys. Fluids,* **14,** 466–474.